Air Bubbles Produced by Breaking Wind Waves: A Laboratory Study

PAUL A. HWANG,* Y.-H. L. HSU** AND JIN WU

Air–Sea Interaction Laboratory, College of Marine Studies, University of Delaware, Lewes, Delaware

(Manuscript received 27 February 1989, in final form 12 June 1989)

ABSTRACT

Air bubbles produced by breaking wind waves are measured in a laboratory tank to study bubble clouds produced in freshwater under various wind and wave conditions. Vertical entrainment of bubbles and their size compositions are found to be influenced greatly by wave structures. The significant wave height appears to be the appropriate scaling length for the vertical distribution of bubble concentrations. Their horizontal distribution, on the other hand, correlates well with the group characteristics of waves. Bubble populations on the water surface are influenced by both wind stress and surface wave height; more specifically, they are governed by the Reynolds number incorporating both effects. Other reported field and laboratory data are shown to follow well the functional variations deduced herewith.

1. Introduction

Air bubbles are entrained at the sea surface by breaking waves. These small bubbles in the near-surface ocean are involved in many oceanographic processes, such as marine-aerosol production (Blanchard and Woodcock 1957), gas exchange (Kanwisher 1963; Merlivat and Memery 1983), and propagation and scattering of acoustic waves (Medwin 1974; Farmer and Lemon 1984). Measurements of bubbles in the field were conducted earlier by Blanchard and Woodcock (1957) with a trap in the surf zone. Subsequent field measurements were performed with similar traps (Kolovayev 1976), with a photographic technique (Johnson and Cooke 1979), and with a sonar (Thorpe 1982, 1986); their results were reviewed and reanalyzed by Wu (1981, 1988) to provide basic functional descriptions of the vertical distribution and size spectrum of bubbles in the near-surface ocean. In the meantime, laboratory experiments were conducted in wind-wave tanks by Koga (1982), Baldy and Bourguel (1987), and Baldy (1988). More recently, the spatial distributions of bubbles were studied by Crawford and Farmer (1987) with an upward looking acoustic transducer mounted on a submarine. In most of these studies, properties of surface waves were not explicitly included in the analyses, while the breaking of waves was generally accepted as the major source of bubble production.

In the present study, size distributions of bubbles were obtained at various depths under different wind velocities in a laboratory tank; in addition, surface waves were simultaneously measured. Continuing the earlier effort (Wu 1981, 1988), we have further quantified horizontal and vertical distributions of bubbles in terms of wind and wave characteristics. Some scaling parameters of these distributions are revealed by applying the present laboratory results to field and other laboratory data (Thorpe 1982, 1986; Baldy and Bourguel 1987; Wu 1988).

2. Experiments

a. Experimental conditions

The experiments were conducted with freshwater in the Wind-Wave–Current Research Facility. It is 40 m long and 1 m wide, and has a 55-cm wind tunnel above 75-cm deep water. The measurements were made at the fetch of about 20 m, over a range of wind velocities from 10 to 15 m s^{-1}. The wind-friction velocity, $u_* = (\tau/\rho)^{1/2}$ with τ being the wind stress and ρ the air density, was determined from the logarithmic wind profile (Hsu 1981). Waves in the present facility started to break with bubbles being formed through air entrainment at the wind velocity of 9 m s^{-1}. The surface displacement near the sampling station of bubbles was continuously measured with a capacitance probe, 1 mm in diameter.

The experimental conditions are listed in Table 1, in which U is the reference wind velocity measured at the middle height of the wind tunnel, T is the period of wave component at the spectral peak, and η is the

* Present affiliation: Science and Technology Corp., Hampton, Virginia.

** Present affiliation: Naval Ocean Research and Development Activity, NSTL, Mississippi.

Corresponding author address: Dr. Jin Wu, University of Delaware, Air–Sea Interaction Laboratory, College of Marine Studies, Lewes, DE 19958.

TABLE 1. Summary of experimental conditions and results.

U (m s^{-1})	u_* (cm s^{-1})	T (s)	η (cm)	Re	h (cm)	N_0 (cm^{-3})
10	55	0.60	1.70	467	5.36	4.6
11	68	0.62	1.79	609	5.80	14.4
12	79	0.65	1.92	754	7.64	35.0
13	96	0.65	2.46	1133	9.86	52.0
14	108	0.75	2.50	1368	10.04	62.0
15	120	0.75	2.70	1620	10.80	92.0

root-mean-square water-surface elevation; other variables will be defined when they first appear.

b. Bubble measurements

An optical sensor based on the light-blocking principle, developed by Wu (1977), was used to measure bubbles with a laser placed on the front side, and a light receiver on the back side, of the tank. The laser beam was expanded in order to have a relatively uniform intensity within the sensing area, occupying the central portion of the beam. This technique is based on geometrical optics and neglects light diffraction (Knollenberg 1970). When a bubble crosses the laser beam, the light sensed by the receiver drops to produce a "dark" pulse. The size of bubble can be determined from the height of the pulse. A pin hole was placed in front of the light sensor to provide a sensing area 3 mm in diameter. The latter, therefore, limits the largest bubble to be measured. Consequently, the sampling volume, in the present experiments, consists of a cylinder 1-m long (tank width) and 3 mm in diameter. The probability of multiple bubbles co-existing in the sensing volume, of course, increases with the bubble concentration. With the present sampling volume, such effects will not become significant until the volumetric concentration of bubbles reaches about 10% (Wu 1977); the latter is about one order of magnitude greater than that encountered in our measurements.

c. Data acquisition

Simultaneous measurements of waves and bubbles were performed at approximately 20 m fetch; the bubble sensor was located 3 cm upwind of the wave probe. For each wind velocity, bubble data at ten to fifteen depths were collected. The recorded bubble data were subsequently processed on a pulse height analyzer to produce both the size spectra of bubbles and the time series of their occurrences. For the latter, the wave data were digitized synchronically for comparison.

3. Temporally averaged bubble properties

a. Vertical distribution of bubble populations

1) VERTICAL DISTRIBUTION

For each sequence of bubble measurements at a given depth, a ten-minute recording was processed on the pulse height analyzer. The accumulated (global) bubble populations over the entire size range 800–3000 μm diameter, denoted as $N(z)$, were first obtained. The results under each wind velocity are compiled in Fig. 1, in which the bubble population is seen to follow well the exponential distribution as suggested earlier (Wu 1981). The straight line fitted to the data was then extended to the zero depth to determine the bubble population at the water surface, N_0. Consequently, the vertical distribution of bubble populations can be expressed as (Wu 1981),

$$N(z)/N_0 = \exp(-z/h) \qquad (1)$$

where z is the depth of measurements, and h is a depth characterizing the entrainment of bubbles from the water surface. The entrainment depth, h, was deduced by fitting the above expression to the data in Fig. 1; the results are compiled in Table 1.

2) SCALING PARAMETER

Inasmuch as the entrainment is caused mainly by the breaking waves, the wave height was suggested (Hsu et al. 1984; Thorpe 1986; Baldy and Bourguel 1987) as the length scale governing the entrainment of bubbles. Recently, observations on the wave breaking were performed in the same facility (Xu et al. 1986; Hwang et al. 1989). The breaking events were detected by local instabilities of the wave profile either due to geometric consideration (the local wave slope exceeding a critical steepness), or kinematic consideration (the local par-

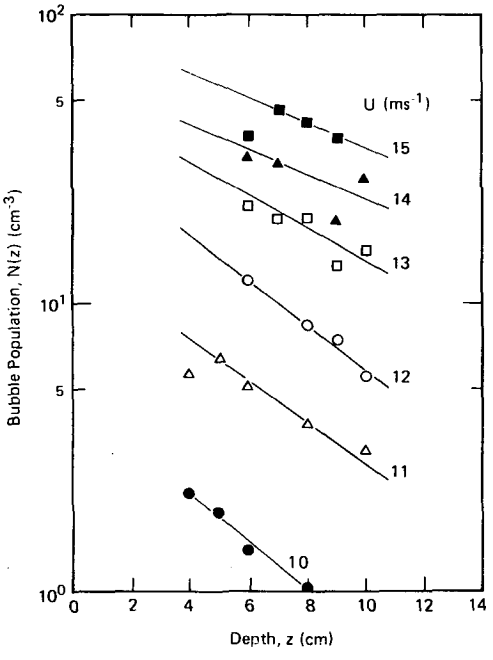

FIG. 1. Vertical distributions of bubble populations at various wind velocities.

TABLE 2. The statistics of the averaged height of breaking waves as a function of the root-mean-square surface elevation. The data are compiled from the wave-breaking experiment reported by Hwang et al. (1989).

U (m s^{-1})	7	8	9	10	11	12	13	14	15	16
H_B (cm)	2.85	3.32	4.04	4.05	5.33	5.97	7.09	7.53	8.72	8.67
η (cm)	0.89	1.14	1.34	1.50	1.76	2.02	2.41	2.57	2.92	3.02
H_B/η	3.20	2.91	3.01	2.70	3.02	2.96	2.94	2.93	2.97	2.87

ticle velocity exceeding the phase velocity of the wave form). In either case, the detaching of surface particles from the water surface is expected. Various parameters, including the vertical and horizontal length scales of breaking waves, were reported by them. Averaged heights of breaking waves, H_B, at various wind velocities obtained from their experiments are shown in Table 2, in which the corresponding root-mean-square water-surface displacement, η, is also presented. There exists a distinctly linear relationship beween H_B and η, elucidated by the narrow range of the ratio H_B/η shown in the last row of the table. The significant wave height, $H_s = 4\eta$, is generally chosen in most studies as the representative wave parameter; it is therefore also selected herewith as the vertical length scale. Statistically, H_s is equivalent to the averaged height of the largest one-third waves. It is shown in Table 2 that H_B is less than H_s, with $H_B/\eta < 4$. This indicates that in a random wave field, the waves that break due to local instabilities are not necessarily the highest waves; the latter are usually longer, and are also geometrically or kinematically more stable.

The normalized bubble populations are presented versus the ratio between the measurement depth and significant wave height in Fig. 2. The solid line in the figure corresponds to Eq. (1) with $h = H_s$. All the data are now seen to collapse onto the same normalized distribution.

The quasi-linear relationship between the entrainment depth and the significant wave height of our laboratory results is also shown in Fig. 3, in which reported field results (Thorpe 1982; Johnson and Cooke 1979) are also compiled. Since no wave information was provided by these authors, we have estimated the significant wave heights from their reported wind and fetch, based on the model of Sverdrup–Munk–Bretschneider (CERC 1973). Using an acoustic transducer, Thorpe (1982) investigated the entrainment of bubbles in the field. He showed that the depth of bubble plumes varied linearly with wind velocity, and the vertical distribution of acoustic cross section was exponential. The entrainment depth calculated from Thorpe's measurements also shows a near linear dependence on the estimated wave height (Fig. 3). The result of Johnson and Cooke (1979), also presented in Fig. 3, is seen again to follow a similar linear trend. More recently, Thorpe (1986) reported acoustic bubble measurements obtained from the Irish Sea in March 1984 and on the edge of continental shelf off the coast of England (Station DB2) during fall (September–October 1984) and winter (December 1984–February 1985) seasons. In this study, data on wind, waves and temperatures were also simultaneously collected. We have divided his data into three groups, and listed the representative environmental conditions in Table 3.

It is found that there are distinct differences among these three datasets, shown in Fig. 3. The data collected from the Irish Sea display a similar linear relationship between entrainment depth and wave height; see inset in Fig. 3. The data from DB2 are more scattered and show a noticeably reduced entrainment as compared to the other datasets; the effects appear to be more pronounced for the winter observations. Interestingly enough, despite of this reduced entrainment as observed from the vertical distribution of acoustic backscatter cross sections, the averaged depth of bubble clouds was found to be deeper in DB2 than that in the Irish Sea, which in turn is deeper than the observations made in the Oban Sea (p. 1466, Thorpe 1986).

In summary, the laboratory and field data compiled in Fig. 3 illustrate a generally linear variation between the entrainment depth and the significant wave height.

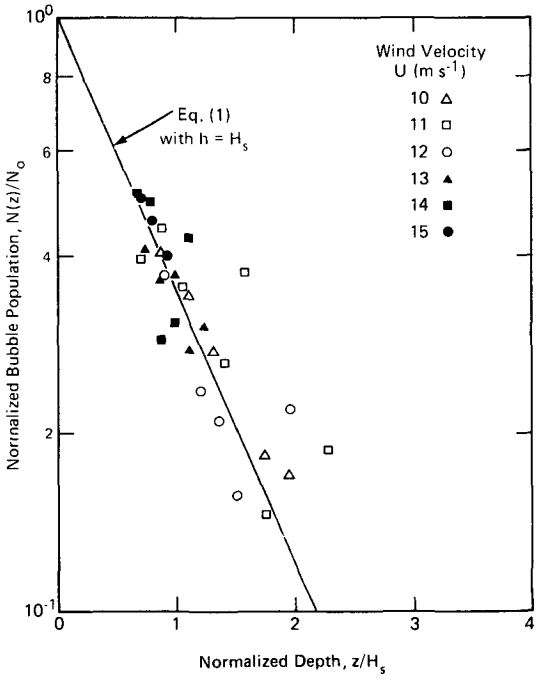

FIG. 2. Normalized vertical distributions of bubble populations at various wind velocities.

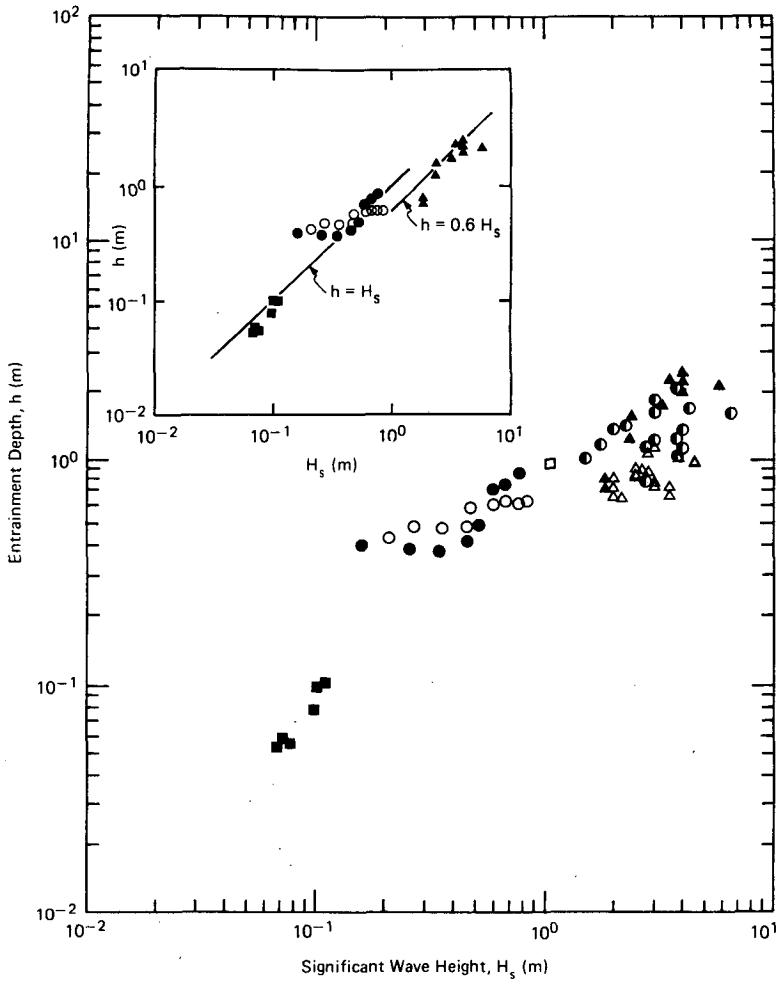

FIG. 3. Variations of bubble entrainment depth with significant wave height. The data are from Johnson and Cooke (1979) □; Thorpe (1982): ○ (Loch Ness) and ● (Oban Sea); Thorpe (1986): ▲ (Irish Sea), ◐ (DB2 Fall) and △ (DB2 Winter); and present study ■.

Overall, they appear to confirm that the vertical entrainment of bubbles can be scaled according to the wave height,

$$h = \beta H_s \qquad (2)$$

where β is of order one and appears to decrease with fetch. Deviations of the field data from the linear relationship at low wind velocities (data points with H_s < 50 cm) can be attributed to different mechanisms of the bubble production, such as through subsurface biological or geological processes. Other sources of acoustic noises not related to bubble plumes may also become relatively more significant under these low-wind conditions with less active wave breaking. In the open ocean, h is less than H_s and with considerable seasonal variations. The exact mechanism and a quantitative description of temperature effects on bubble generation are not clear at this stage. The observations of a related phenomenon, the whitecap coverage in the ocean, do suggest, however, a reduced whitecap coverage at lower seawater temperature (Wu 1988). From the above discussion, it is clear that wave breaking has a definite effect on the bubble entrainment process,

TABLE 3. Summary of the environmental conditions in Thorpe's (1986) experiments. The number in parentheses represents the number of data points in each category.

	Irish Sea	DB2 Fall	DB2 Winter
Wind (m s^{-1})	7.3–14.1	6.9–14.4	7.3–14.4
Water depth (m)	?	167	167
Fetch (km)	>140 (8) < 30 (2)	>330 (17)	>625 (17) 350 (1)
Sea water temperature	6–7 (4) 16–17 (6)	14.7–17	10.7–11.6
Stability	Mostly unstable	Unstable to mildly stable	Unstable to mildly stable

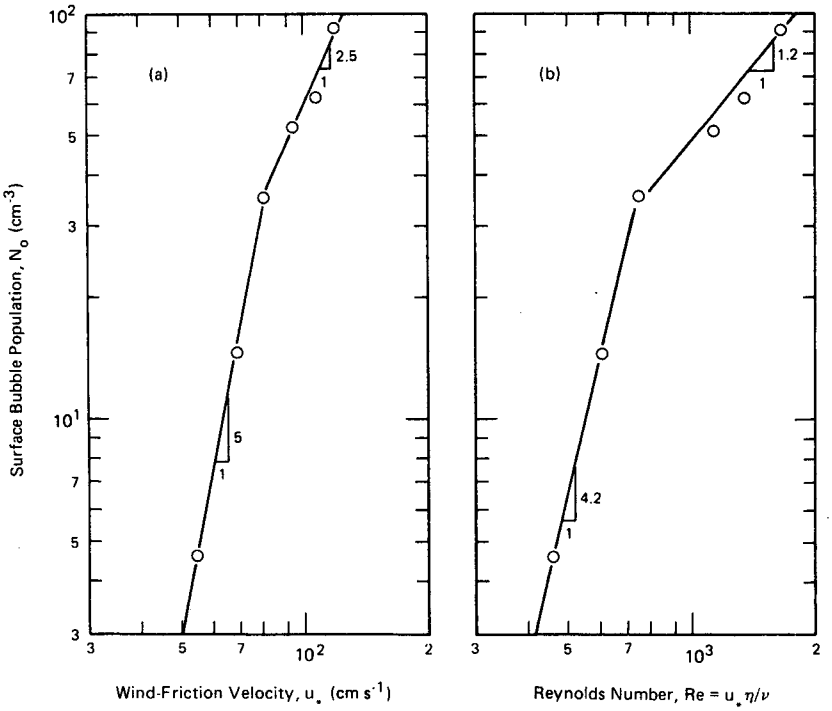

FIG. 4. Increase of bubble population at the water surface with wind-friction velocity and Reynolds number.

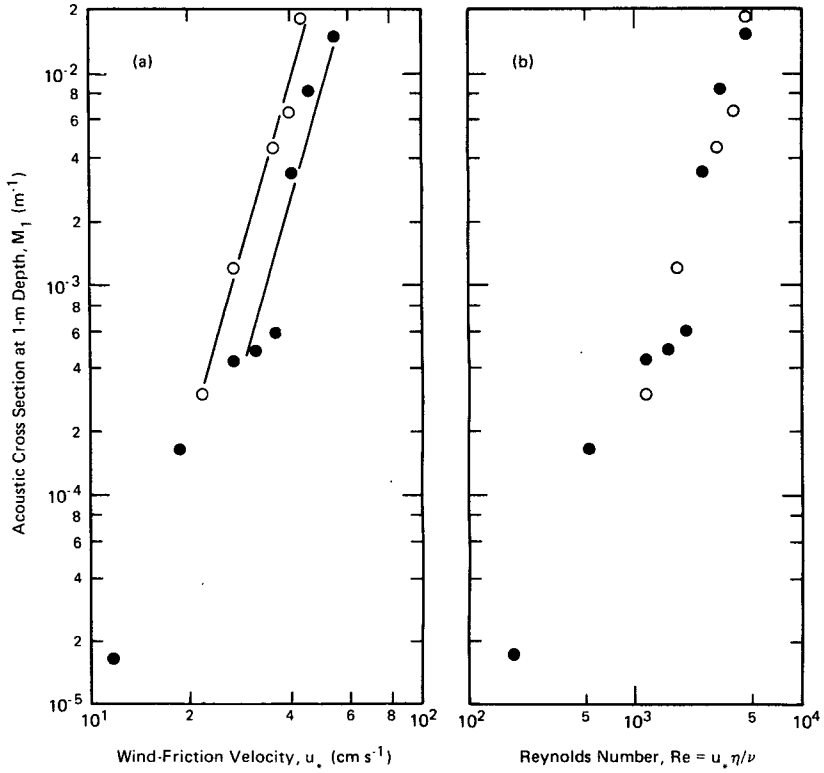

FIG. 5. Variations of the acoustic cross section at 1-m depth with the wind-friction velocity and Reynolds number. The data were obtained by Thorpe (1982) at long (○) and short (●) fetches.

and the breaking wave height is an important parameter to quantify such an effect.

b. *Bubble population at water surface*

1) VARIATION WITH WIND-FRICTION VELOCITY

Bubble population at the water surface under various wind velocities are presented in Fig. 4a. In agreement with Wu (1981, 1988), the increase of water-surface bubble population with the wind-friction velocity is seen to follow a power law. The exponents of the power law, however, differ at low and high winds. At low winds ($u_* < 80$ cm s^{-1}), the exponent is close to 5, indicating a very rapid increase of the surface bubble population with the wind velocity. For high winds ($u_* > 80$ cm s^{-1}), the rate of increase becomes more gradual; the exponent is about 2.5. These relationships can be expressed as

$$N_0 \sim \begin{cases} u_*^5, & u_* < 80 \text{ cm s}^{-1} \\ u_*^{2.5}, & u_* > 80 \text{ cm s}^{-1}. \end{cases} \quad (3)$$

Such a change of the dependence on wind-friction velocity is believed to be related to conditions of wave breaking. The frequency of occurrence of wave breaking in the same facility was found to be proportional to $u_*^{2.2}$ for $u_* < 80$ cm s^{-1}, and to u_* for $u_* > 80$ cm s^{-1} (Xu et al. 1986; Hwang et al. 1989). In this case, the exponent at low winds is also about twice that at high winds. These consistent results further substantiate the important influence of surface-wave conditions on quantifying the production of bubbles.

2) VARIATION WITH REYNOLDS NUMBER

Considering that the breaking event is governed by both wind and waves, we define a dimensionless parameter incorporating both factors in the form of the Reynolds number, $\text{Re} = u_*\eta/\nu$, where ν is the kinematic viscosity of air. The data of the bubble population at the water surface are replotted versus this parameter in Fig. 4b, from which the following expressions are deduced:

$$N_0 \sim \begin{cases} \text{Re}^{4.2}, & \text{Re} < 750 \\ \text{Re}^{1.2}, & \text{Re} > 750. \end{cases} \quad (4)$$

Thorpe (1982) presented in his Fig. 9 the acoustic cross sections measured at 1-m depth (M_1) from the Oban site in two different fetch groups. His results are replotted versus the wind-friction velocity in Fig. 5a. The friction velocity is calculated from the wind velocity using the formula of wind-stress coefficients proposed by Wu (1985). There is a factor of three difference between the data obtained from the longer (greater than 13.6 km) and the short (less than 5.7 km) fetches, as illustrated by the lines fitting to these two groups of data. When they are plotted versus the Reynolds number in Fig. 5b, the two groups tend to merge together. This offers a clear support of the scaling with the Reynolds number incorporating influences of both wind and waves.

c. *Size spectrum of air bubbles*

1) FORM OF SIZE SPECTRUM

A sample set of bubble size spectra obtained at various depths under $U = 14$ m s^{-1} is shown in Fig. 6. On the large-size side of the spectral peak, the bubble population is seen to decrease rapidly as the diameter increases and follows generally a power law (Wu 1981),

$$n(d) \sim d^{-\alpha} \quad (5)$$

where $n(d)$ is the bubble population per size band, d is the bubble diameter, and α is the slope of the size spectrum.

The bubble-size spectra obtained at other wind velocities are not presented here, as they followed a similar trend as those shown in Fig. 6. The spectral slopes do

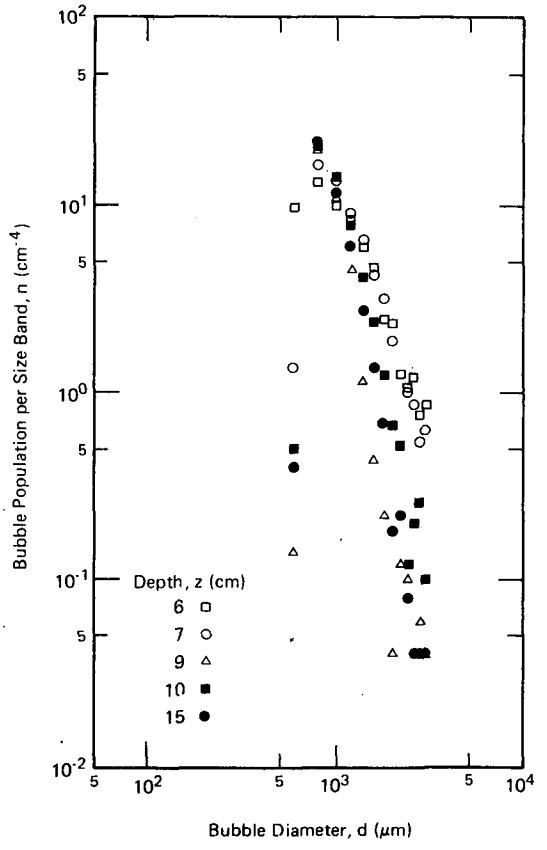

FIG. 6. Sample bubble spectra measured at various depths. The data were obtained at $U = 14$ m s^{-1}.

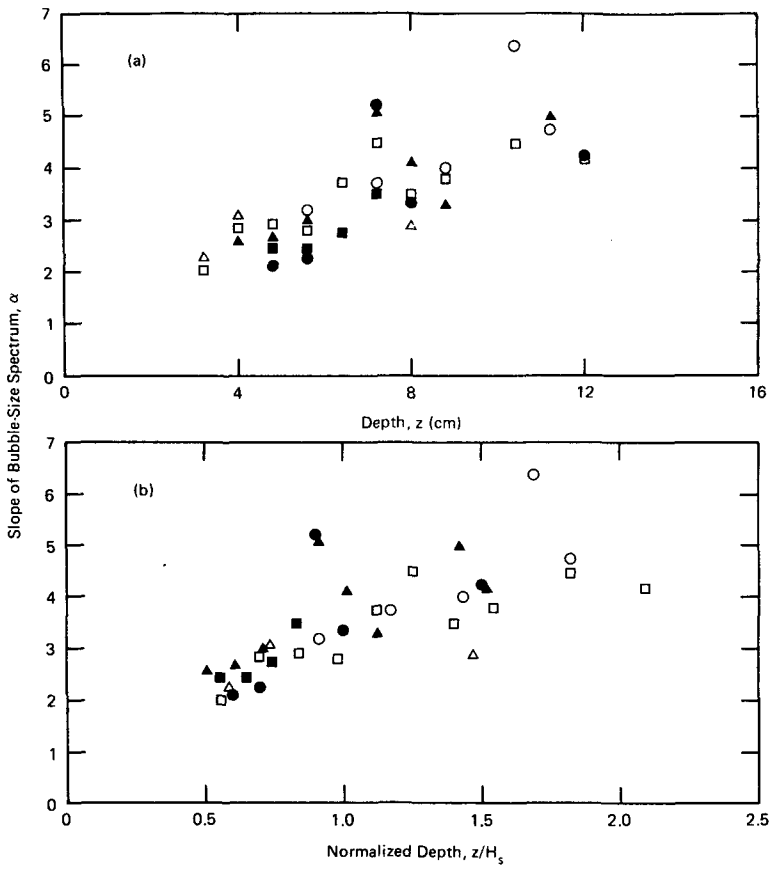

FIG. 7. Slopes of bubble-size spectra at absolute (a) and normalized (b) depths. The symbols used for different wind velocities are the same as those in Fig. 2.

not appear to vary systematically with wind velocity; their variation with depth is discussed in the following.

2) VARIATION OF SPECTRAL SLOPES

The spectral slopes obtained at various depths under different wind velocities are presented in Fig. 7a versus the depth of measurements. The trend is clear at all wind velocities, displaying a steepening of the bubble size spectrum with the depth. Following the discussion presented in the previous section, the significant wave height is again used for the vertical scaling. The spectral slope α was then plotted versus the normalized depth z/H_s in Fig. 7b, and is seen to increase almost linearly up to $z/H_s = 1.2$. Below this normalized depth, the spectral slope remains nearly constant, being approximately 4. Near the water surface, the data display the following linear relationship

$$\alpha = 2.8z/H_s + 0.7, \quad 0.5 < z/H_s < 1.2. \quad (6)$$

In oceanic conditions, bubble size spectra appear to be universal at various depths under different wind velocities (Wu 1981), having a spectral slope of about 4 (Wu 1988). The universal slope deduced from the field data differs little from those at large depths shown in Fig. 7b.

4. Temporally varied bubble properties

a. Correlation with wave structures

As discussed earlier, the recorded signals produced by the bubbles are time series of pulses. By using the accumulation mode of the pulse height analyzer, the number of bubbles in the sensing volume accumulated over a predetermined time interval (1/10 s) could be obtained. The wave data were also simultaneously digitized at the same rate (10 Hz); a distinct grouping structure was detected. The typical number of waves in each group was in the order of 10 with a factor of two variation. The temporal distribution of bubble occurrences appears to be associated more closely with the grouping structure than with the instantaneous surface undulation. In order to illustrate this feature, we performed the following analyses.

The time sequence of bubble numbers accumulated over intervals of 1/10 s was found to be still spurious,

a low-pass procedure was then adopted for smoothing. Using the wave period (defined by zero-crossings of the wave record) as a time unit, two new time series: the wave height and the number of bubbles in each wave period, were finally generated. The cross correlations between these two time series were subsequently calculated. The correlation coefficients between the wave height and bubble occurrence obtained under various wind velocities are shown in Fig. 8. Despite small values of the correlation coefficient, the periodic feature of the function is quite obvious. Time lags between the primary and secondary peaks of the correlation function are approximately 10 to 20 wave periods, with a weak dependence on the wind velocity. This time lag between two peaks of the correlation function is consistent with observations of the wave grouping discussed above.

At higher wind velocity, the bubble signals are less spurious, we attempted to compute the bubble frequency spectrum using a 384-s data segment collected at the wind velocity of 13 m s^{-1} and sampled at 1/10-s intervals. The results are presented in Fig. 9b, while for reference the wave spectrum is presented in Fig. 9a. The high-frequency portion ($f > 1/12.8$ s^{-1}) of the spectrum, shown as the solid curve in Fig. 9b, is an ensemble average of thirty data segments, each 12.8-s long (the degree of freedom is 60). The low-frequency portion, the dashed curve in Fig. 9b, is the averaged

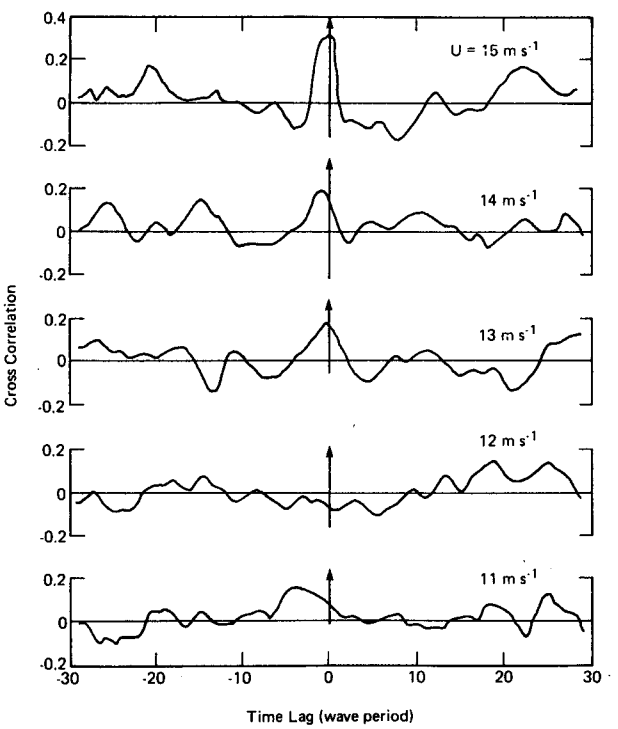

FIG. 8. Correlation of bubble populations and wave heights at various wind velocities.

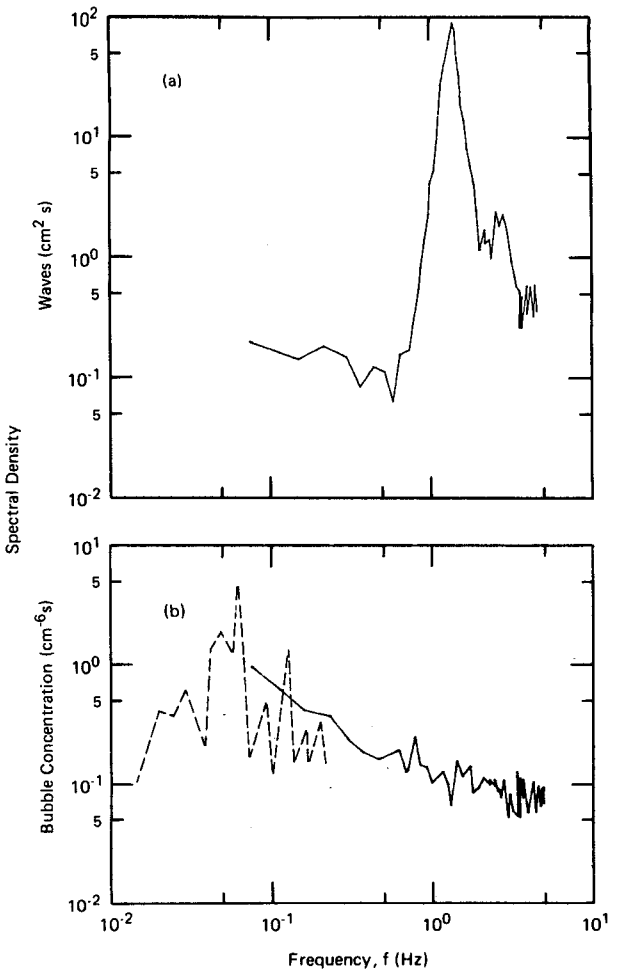

FIG. 9. Comparison of spectra of waves (a) and bubble occurrences (b). The data were obtained at the wind velocity of 13 m s^{-1}, and the bubbles were measured at $z = 6$ cm.

spectrum computed from three 102.4-s data records (the degree of freedom is 6). The size range of the cumulated bubbles is 1000 to 3000 μm in diameter. The corresponding wave-height spectrum is seen in Fig. 9a to have its peak frequency, f_p, at 1.54 Hz. The dominant peak of the bubble frequency spectrum, however, is at a considerably lower frequency, approximately $0.05 f_p$ (Fig. 9b). These spectral characteristics again substantiate wave-grouping effects on the bubble distribution, being consistent with those observed from the time records and the correlation analysis displayed in Fig. 8.

b. Comparison with field observations

Crawford and Farmer (1987) presented the frequency spectra of bubbles in the near-surface ocean measured with an acoustic transducer mounted on a submarine. The range of wind velocities during their experiments was between 8 and 11 m s^{-1}; and the

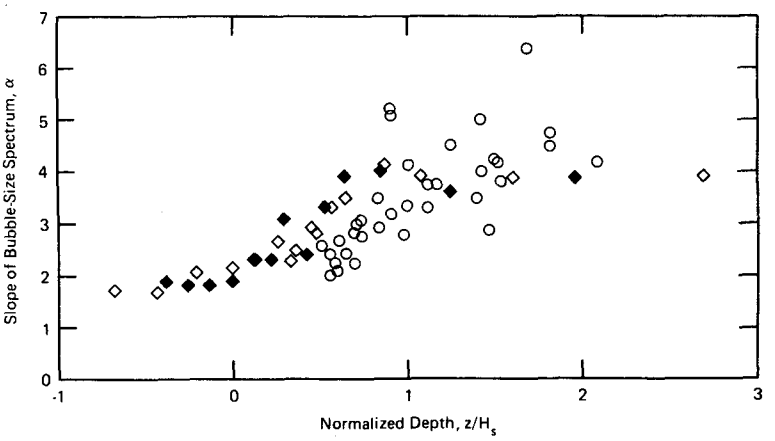

FIG. 10. Comparison of size-spectral slopes obtained in various experiments. They are from present study with wind waves having wind velocities of 10–15 m s^{-1} (○); and those from Baldy and Bourguel [1987] with wind waves (◇) and with wind waves superimposed on mechanical waves (◆), both at the wind velocity of 14 m s^{-1}.

range of bubble sizes measured was from 60 to 280 μm. For these somewhat smaller bubbles, they also observed a weak spectral peak at the second subharmonic of the wave spectrum, and related its presence of this weak peak to the features of breaking waves and the associated group structure as reported by Donelan et al. (1972).

5. Discussions

a. Further comparison with other laboratory data

Baldy and Bourguel (1987) and Baldy (1988) extended their measurements of bubbles closer to the water surface to include the region between the wave crest and trough. They also reported similar shapes of the bubble size spectrum and a linear increase of the spectral slope with the depth of measurements. Their data indicate that this linear region may extend to $z/H_s < 0.5$, which is above the wave trough. They further showed that above the mean water level ($z/H_s < 0$) and below one wave height ($z/H_s > 1$), the slopes of the size spectra have nearly constant values of 2 and 4, respectively. The present results and the data reported in Baldy and Bourguel (1987), which includes data discussed in Baldy (1988), are compared in Fig. 10. A general agreement is shown between these two sets of results, except perhaps in the depth range $0.5 < z/H_s < 1.0$. Taking together all available data shown in Fig. 10, we now see that the linear dependence of the spectral slope on the normalized depth exists within the region $0 < z/H_s < 2.0$.

b. Further comparison with reported field data

Vertical distributions of acoustic cross sections obtained by Thorpe (1982) at Oban and Loch Ness were extrapolated to determine the surface values (M_0). His results along with surface bubble populations (N_0) from the present laboratory experiment are plotted versus corresponding Reynolds numbers in Fig. 11. The acoustic cross section is proportional to the bubble size and the number of bubbles in each size range. Since the size composition of bubbles was shown to be relatively universal near the water surface (Figs. 7 and 10), it is expected that dependencies of M_0 and N_0 on external wind and wave conditions are similar. Such a similarity is indeed observed in Fig. 11. In the high Reynolds number range (Re > 1000), both M_0 and N_0 increase at a rate of approximately $\mathrm{Re}^{1.2}$, as illustrated by short straight lines in the figure. At low Reynolds numbers, the steeper rate of increase observed from the laboratory data, as shown in Fig. 4, was not found among sets of field data. This difference in characteristics at low Reynolds numbers is probably related to the difference in breaking-wave characteristics in laboratory tanks and the ocean. It may also be caused by other sources of bubble generations and acoustic noises, not related to the wind, becoming relatively more important in the acoustic measurements at low wind velocities in the field, as mentioned earlier.

6. Conclusion

Wave breaking is the major mechanism introducing air bubbles into the near-surface water column, therefore, it is expected that the surface wave properties have definite effects on distributions of bubbles in the near-surface water. In this article we reported the results of an experiment, in which simultaneous measurements of bubbles and waves were performed. The analyses confirm that: 1) the significant wave height character-

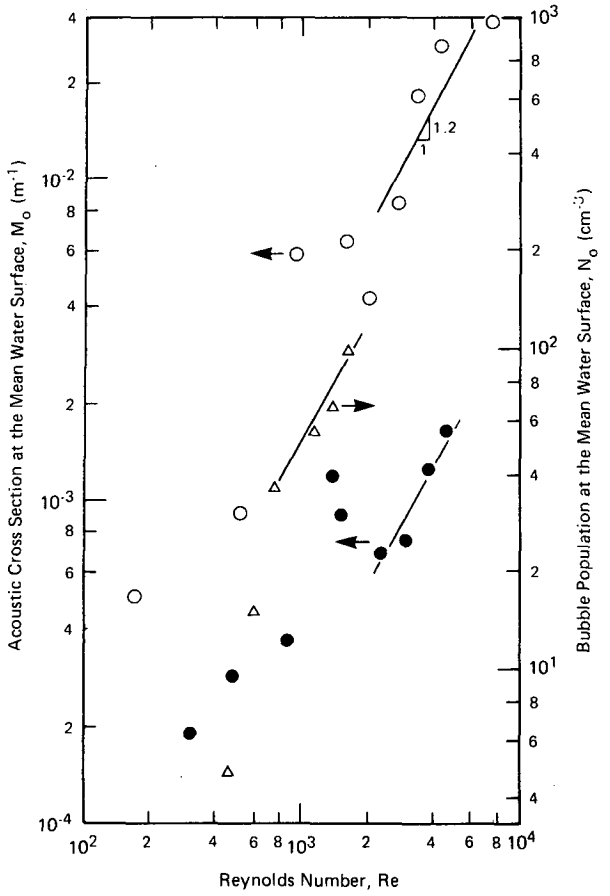

FIG. 11. Reynolds number scaling of the acoustic cross section and bubble population at the water surface. The acoustic data are deduced from Thorpe's (1982) measurements at Oban Sea (○) and Loch Ness (●); the bubble data (△) are from the present experiment.

izes the vertical structure of bubble distributions, including the bubble entrainment from the water surface, and the vertical variation of bubble size spectra; 2) the wave grouping affects the longitudinal distribution of bubbles; and 3) both wind stress and wave conditions affect the bubble population at the air–water interface, these two parameters can be combined into a nondimensional quantity in the form of Reynolds number. Our results are also substantiated by field and other laboratory measurements.

Acknowledgments. We are very grateful for the support of this work provided by the Fluid Dynamics Program (Grant N00014-89-J-1100) and the Ocean/Atmospheric/Polar Environments Program (Contract N00014-87-K-1557), Office of Naval Research.

REFERENCES

Baldy, S., 1988: Bubbles in the close vicinity of breaking waves: Statistical characteristics of the generation and dispersion mechanism. *J. Geophys. Res.*, **93,** 8239–8248.

——, and M. Bourguel, 1987: Bubbles between wave trough and wave crest levels. *J. Geophys. Res.*, **92,** 2919–2929.

Blanchard, D. C., and A. H. Woodcock, 1957: Bubble formation and modification in the sea and its meteorological significance. *Tellus,* **9,** 145–158.

CERC (Coastal Engineering Research Center, U.S. Army), 1973: Shore Protection Manual, Vol. XX.

Crawford, G. B., and D. M. Farmer, 1987: On the spatial distribution of ocean bubbles. *J. Geophys. Res.*, **92,** 8231–8243.

Donelan, M. A., M. S. Longuet-Higgins and J. S. Turner, 1972: Periodicity in whitecaps. *Nature,* **234,** 449–451.

Farmer, D. M., and D. D. Lemon, 1984: The influence of bubbles on ambient noise in the ocean at high wind speeds. *J. Phys. Oceanogr.*, **14,** 1762–1778.

Hsu, Y.-H. L., 1981: Turbulent transfers in the atmospheric surface layer under various stability conditions—A laboratory study. Ph.D. dissertation, University of Delaware.

——, P. A. Hwang and Jin Wu, 1984: Bubbles produced by breaking wind waves. "*Gas Transfer at Water Surfaces,*" W. Brutsaert and G. H. Jirka, Eds., D. Reidel, 221–227.

Hwang, P. A., Delun Xu and Jin Wu, 1989: Breaking wind waves: Measurements and characteristics. *J. Fluid Mech.*, **202,** 177–200.

Johnson, B. D., and R. C. Cooke, 1979: Bubble populations and spectra in coastal waters: A photographic approach. *J. Geophys. Res.*, **84,** 3761–3766.

Kanwisher, J., 1963: On the exchange of gases between the atmosphere and the sea. *Deep-Sea Res.*, **10,** 195–207.

Knollenberg, R. G., 1970: The optical array: An alternative to scattering or extinction for airborne particle size determination. *J. Appl. Meteor.*, **9,** 86–103.

Koga, M., 1982: Bubble entrainment in breaking wind waves. *Tellus,* **34,** 481–489.

Kolovayev, P. A., 1976: Investigation of the concentration and statistical size distribution of wind-produced bubbles in the near-surface ocean layer. *Oceanology,* (Engl. Transl.), **15,** 659–661.

Medwin, H., 1974: Acoustic fluctuations due to microbubbles in the near-surface ocean. *J. Acoust. Soc. Am.*, **56,** 1100–1104.

Merlivat, L., and L. Memery, 1983: Gas exchange across an air–water interface: Experimental results and modeling of bubble contribution to transfer. *J. Geophys. Res.*, **88,** 707–724.

Thorpe, S. A., 1982: On the clouds of bubbles formed by breaking waves in deep water and their role in air–sea gas transfer. *Phil. Trans. Roy. Soc. London,* **A304,** 155–210.

——, 1986: Measurements with an automatically recording inverted echo sounder; ARIES and the bubble clouds. *J. Phys. Oceanogr.*, **16,** 1462–1478.

Wu, Jin, 1977: Fast-moving suspended particles: Measurements of their size and velocity. *App. Optics,* **16,** 596–600.

——, 1981: Bubble populations and spectra in near-surface ocean: Summary and review of field measurements. *J. Geophys. Res.*, **86,** 457–463.

——, 1985: Parameterization of wind-stress coefficients over water surface. *J. Geophys. Res.*, **90,** 9069–9072.

——, 1988: Bubbles in the near surface ocean: A general description. *J. Geophys. Res.*, **93,** 587–590.

——, 1988: Variation of whitecap coverage with wind stress and water temperature. *J. Phys. Oceanogr.*, **18,** 1448–1453.

Xu, Delun, P. A. Hwang and Jin Wu, 1986: Breaking of wind-generated waves. *J. Phys. Oceanogr.*, **16,** 2172–2178.